Final version of this article is published by NRC Research Press and available at: http://dx.doi.org/10.1139/O2012-029

Partial Oligomerization of Pyolysin Induced by a Disulfide-Tethered Mutant

Clara Baik[ab], Lisa Pokrajac[ab], J. Robin Harris[cd], Stephen J. Billington[e], Michael Palmer[af]

[c]Institute for Cell and Molecular Biosciences, University of Newcastle, Newcastle-upon-Tyne, UK.

[d]Institute of Zoology, University of Mainz, 55099 Mainz, Germany

[a]Department of Chemistry, University of Waterloo, 200 University Ave. W., Waterloo, Ontario, N2L 3G1, Canada

[e]Department of Veterinary Science and Microbiology, The University of Arizona, 1117 East Lowell Street, Tucson, AZ 85721, USA

[f]Corresponding author. Email: mpalmer@uwaterloo.ca

[b]These authors contributed equally to this work.

Summary

The bacterial toxin pyolysin (PLO) belongs to the family of Cholesterol-Dependent Cytolysins (CDCs), which form large, oligomeric pores in cholesterol-containing membranes. Monomeric CDC molecules have a structure of four domains, with domains 2 and 3 packed against each other. After binding to target membranes containing cholesterol, toxin monomers oligomerize into pre-pore complexes. Trans-membrane pores form when the pre-pores insert into the lipid bilayer. Membrane insertion requires each subunit in the pre-pore to undergo a significant change in conformation, including the separation of domains 2 and 3. We here describe a pyolysin mutant with an engineered disulfide bond between domains 2 and 3 that is unable to complete this conformational change and thus does not form pores. In contrast to a similar mutant previously described for the homologous toxin perfringolysin O, the disulfide-tethered mutant does not form pre-pore oligomers, indicating that it is already inhibited at the stage of oligomerization. When mixed with wild type PLO, the mutant partially inhibits oligomerization of the latter, so that the resulting hybrid oligomers are reduced in size and arc-shaped rather than ring-shaped. Osmotic protection experiments indicate that such oligomers can form functional pores of reduced size. These findings indicate that conformational flexibility between domains 2 and 3 is required for oligomerization. Moreover, membrane insertion can be triggered in oligomers that contain some insertion-deficient subunits and is therefore only partially cooperative.

Introduction

Arcanobacterium pyogenes is a Gram-positive bacterial pathogen of livestock. An important virulence factor of *A. pyogenes* is the cytolytic toxin pyolysin (PLO). This toxin is a member of the large group of toxins known as the Cholesterol Dependent Cytolysins (CDC), which take their name from their absolute dependence on cholesterol in the target membrane for activity. These toxins form exceptionally large oligomeric trans-membrane pores (1), which consist of 40-50 monomers and have diameters of up to 30 nm (2).

Crystallographic studies on other members of the CDC family, namely perfringolysin O (PFO) and intermedilysin (ILY) show that the monomeric toxin molecule is elongated and contains four domains rich in β-sheet structure (3; 4). Upon binding to a target membrane, molecules diffuse laterally on the surface, interact with other bound CDC monomers, and form a pre-pore complex (5). Subsequently, a profound conformational change occurs that results in the formation of the trans-membrane pore (6). During this change, domain 2 dissociates from domain 3, whereupon two initially α-helical segments in domain three change shape into β-hairpins and become deeply inserted into the membrane (7).

In a previous study on the homologous toxin perfringolysin O, it had been reported that introduction of a disulfide bond between domains 2 and 3 prevented membrane insertion, while still allowing the assembly of pre-pore oligomers (8). This observation suggests that conformational flexibility of domain 2 relative to domain 3 is not required up to the pre-pore stage. We here report that a homologous disulfide mutant derived from the homologous toxin pyolysin fails to oligomerize. The mutant also interferes with the activity of wild type PLO in a dose-dependent manner. At large molar excess over the latter, inhibition of hemolysis is virtually complete, whereas at equimolar ratio hemolysis is partially preserved, but both oligomer and pore size is reduced. These findings indicate that conformational flexibility between domains 2 and 3 is required for proper oligomerization. Furthermore, they show that membrane insertion of oligomers is cooperative, yet completion of oligomerization to ring shape is not necessary.

Materials and Methods

Construction, Expression and Purification of PLO Mutants. The mutants created for this investigation were based on on the plasmid pJGS59 (9) encoding the PLO wild type gene, fused to an N-terminal hexa-histidine purification tag. Site directed mutagenesis was performed according to (10). Introduction of mutations, and absence of any unintended second site mutations was confirmed by DNA sequencing (McMaster University, ON). For expression, the mutant plasmids were transformed into *E. coli* BL21 and cultured in 2xYT broth supplemented with 0.5mM IPTG (BioShop, Burlington ON) for protein expression. After harvesting, cells were lysed using a Emulsiflex C5 Emulsifier (Avestin, Ottawa ON) and the protein was purified using a BioRad Biologic LP liquid chromatography system (Mississauga ON) with a nickel agarose column (Qiagen, Mississauga ON).

Chemical Modification of Cysteine Residues. Protein samples were transferred to labelling buffer consisting of 50mM Tris, 150 mM NaCl, 1mM EDTA (BioShop, Burlington ON) pH 7.5 using gel filtration. The single cysteine mutants were supplemented to 1 mM of either Fluorescein-5-Maleimide (Biotium Inc, Hayward CA), Rhodamine Red Maleimide or N,N'-dimethyl-N-(iodoacetyl)-N'-(7-nitrobenz-2-oxa-1,3-diazol-4-yl)ethylenediamine (IANBD; both from Invitrogen, Burlington ON). The samples were incubated at 25ºC for 60 minutes and excess label was removed using gel filtration chromatography. Labelling efficiencies of 85-90% for fluorescein and 70-80% for rhodamine an IANBD were obtained, as determined by UV-Vis absorbance and extinction coefficients of 83,000 $M^{-1}cm^{-1}$ for fluorescein, 91,000 $M^{-1}cm^{-1}$ for rhodamine and 24 667 $M^{-1}cm^{-1}$ for IANBD.

Preparation of Red Blood Cells and Ghost Membranes. For hemolysis assays, aliquots of 400 µl sheep red blood (Cedarlane, Burlington, ON) cells were diluted to 1 ml with PBS buffer (16mM K_2HPO_4, 150mM NaCl, 1mM EDTA, pH 7.5), centrifuged in a tabletop centrifuge for 4 minutes, and the supernatant removed to yield a 100 µl RBC pellet. The pellet was washed with PBS buffer by centrifugation until the supernatant remained clear. The pellet was resuspended again to a final volume of 1 ml to a concentration of 10%. From this, 1% RBC working solutions were made. To prepare ghost membranes, 400 µl sheep RBC were mixed with 600 µl cell lysis buffer (5 mM NaCl, 5 mM Na_2HPO_4 pH 7.0) and centrifuged at 13,000 rpm for 10 minutes. The

supernatant was removed and the pellet washed until both the supernatant became clear and the pellet translucent. The pellet was made up to 1 ml with PBS buffer.

Hemolysis Assay. Two-fold serial dilutions were made of PLO-DS (initial concentration 30 μg/ml) in a 96-well plate with PBS buffer, in the presence and absence on 5 mM dithiothreitol (DTT; BioShop, Burlington ON). Sheep red blood cells were added to each well to a final concentration of 0.5% and incubated at 37 ºC for 30 minutes. The decrease in cell turbidity corresponding to hemolysis was monitored at a wavelength (650 nm) outside the absorbance of hemoglobin, using a SpectroMax Plus 384 Microplate Spectrophotometer (Molecular Devices, Sunnyvale CA). Wild type PLO (30ug/ml) was admixed with PLO-DS to ratios of 1:1, 1:2, 1:4, 1:8 and 1:12 and tested for hemolytic activity as above.

Fluorescence Spectroscopy. All samples containing labelled protein were made to a final concentration of 1 μM, with 1% (v/v) of red cell ghost membranes. For all fluorescence assays, fluorescein- and rhodamine- labeled toxin was combined in a 1:1 ratio (0.5 μM each). Steady state fluorescence spectra were recorded on a PTI QuantaMaster spectrofluorimeter using an excitation wavelength of 465 nm with emission scans recorded from 495 to 620 nm, using 2 mm excitation and emission slit widths. The labeled toxin samples were incubated with ghost membranes to a final membrane concentration of 1% (v/v) and incubated at 37 ºC for 30 minutes. The membranes were then collected by centrifugation and resuspended in buffer. Spectra were subtracted with erythrocyte ghost suspension as a blank.

Time-resolved fluorescence was measured using an FT-100 compact fluorescence lifetime spectrometer (PicoQuant, Berlin, Germany) using an LDH-P-C-470 LED laser light source. Fluorescein emission was isolated using a 520±5nm bandpass filter (Andover, Salem, NH). Decays were fitted using FluoFit software (PicoQuant) fitting to three lifetime components from which the average lifetime $<\tau>$ was calculated, using the formula

$$\tau \geq \frac{\Sigma \alpha_i \tau_i}{\Sigma \alpha_i}$$

where α_i represents the amplitude at time zero and τ_i is the lifetime of the i^{th} component. All lifetime decay values were fitted to χ^2 values ≤ 1.2.

Size Exclusion Chromatography. In order to determine relative sizes of hybrid oligomer complexes formed, samples of labeled PLO-R219C-F were made to 1 μM concentration, with an equal amount of unlabeled PLO-DS. Ghost membranes were added to a final concentration of 20% (v/v). Samples were incubated at 37 ºC for 30 minutes, centrifuged at 13,000 rpm for 10 minutes, after which the supernatant was removed. Membranes were dissolved using 5% sodium deoxycholate, and the samples were made to a final volume of 1ml. Size exclusion chromatography was performed on a BioRad BioLogic FPLC (described in Protein Expression and Purification section) using a Sephacryl S-400 column equilibrated with elution buffer consisting of 20 mM Tris, 150mM NaCl, 1 mM EDTA and 0.25% (w/v) sodium deoxycholic acid (BioShop, Burlington ON) pH 8.5. Eluted fractions were collected and analyzed for fluorescein fluorescence.

Osmotic Protection Assay. A standard buffer of 10 mM K_2HPO_4, 25mM NaCl at pH 7.5 was supplemented with either Dextran 6 to 13% (w/v) or Dextran 40 (both, Fluka BioChemika, Switzerland) to 17% (w/v). Washed sheep erythrocytes were suspended in the above buffers to a final concentration of 0.5%. The suspension was dispensed into the wells of a microtitre plate and supplemented with 2.5 μg/ml of wild type PLO either alone, or supplemented with the same amount or twice the amount of PLO-DS. The time course of hemolysis was followed during incubation at 25 ºC for 30 minutes by measuring the OD at 650 nm in a SpectraMax Plus 384 Microplate Spectrophotometer.

Transmission Electron Microscopy. Wild type PLO and of PLO-DS, alone or in mixtures as indicated in the Results section, were incubated at a total protein concentration of 0.125 mg/ml with cholesterol crystals (0.5 mg/ml, prepared according to (11)) for 30 minutes at room temperature. The samples were subjected to negative staining with 2% uranyl acetate according to (12). TEM study of the negatively stained specimens was performed in a Phillips CM 100 transmission electron microscope at 100 kV. Digital images were recorded using an Optronics 1824x1824 pixel CCD camera with an AMT40 version 5.42 image capture engine, supplied by Deben (Bury St. Edmunds, UK).

Results

Hemolytic Activity of the disulfide-tethered mutant. The hemolytic activity of the disulfide mutant R219C/G85C, or PLO-DS for short. The PLO-DS is shown in Figure 2. Wild type PLO (PLO-WT) exhibits 50% hemolysis at approximately 400 ng/ml. In contrast, PLO-DS shows no hemolytic activity up to a concentration of 30 μg/ml. However, when PLO-DS is reduced with DTT, the hemolytic activity was restored to a level similar to that of wild type pyolysin. This indicates that the functional impairment is due to the disulfide bond and not to the substitutions of residues R219C or G85C individually. These findings are entirely analogous to those reported previously for the homologous mutant of perfringolysin O (8).

PLO-DS does not form oligomers. The disulfide mutant of perfringolysin O was reported to form pre-pores on membranes, with the same circular shape and diameter that also characterizes the final, membrane-inserted perfringolysin pores. In contrast to these prior findings, PLO-DS did not form any distinct, regular ring-shaped oligomers on PC/cholesterol liposome membranes (not shown) or cholesterol crystals (Figure 3A).

Similarly, on cholesterol microcrystals, which provide a minimal but viable model substrate for CDCs (11; 13), the mutant failed to form typical oligomers as illustrated in Figure 3B. Therefore, the mutant is deficient not only in its ability to undergo membrane insertion, but is already unable to properly oligomerize. Oligomerization of the mutant was restored upon reduction with dithiothreitol, which is in agreement with the observed restoration of hemolytic activity.

The lacking oligomerization of PLO-DS is also apparent in fluorescence energy transfer (FRET) experiments. In these experiments, PLO-DS was modeled with the triple mutant PLO R219C/G85C/K328C, which in addition to the disulfide bond contains another cysteine residue amenable to covalent labeling. In both labeled and unlabeled form, the triple mutant functionally behaves like PLO-DS, exhibiting hemolytic activity only upon disulfide reduction with DTT. Wild type toxin was modeled with the single cysteine mutant N90C, which retains hemolytic activity in both labeled and unlabeled form (data not shown).

The mutants were labeled with fluorescein and rhodamine, respectively. Fluorescein and rhodamine form an efficient donor-acceptor pair for FRET, with an R_0 distance of approximately

50 Å (14), which is well above the distance of two adjacent subunits in CDC oligomers (2; 15). Accordingly, when mixtures of fluorescein- and rhodamine-labeled N90C are incubated with membranes, the formation of hybrid oligomers results in a strong reduction of the fluorescein emission (Figure 4A). In contrast, no such reduction is apparent with the triple mutant, indicating absence of oligomerization (Figure 4B).

Effect of PLO-DS on the Oligomerization of Wild Type PLO. When PLO-DS was added to wild type PLO at equal amounts or in slight excess, oligomers were observed, but these were mostly incomplete and arc-shaped, indicating that oligomerization was partially inhibited by the mutant (Figure 3C). With PLO-DS present in tenfold excess, oligomerization was virtually completely inhibited (Figure 3D).

The formation of oligomers of reduced size in equimolar mixtures of PLO-WT and PLO-DS was confirmed with size exclusion chromatography. In these experiments, wild type PLO was replaced with the hemolytically active fluorescein-labeled cysteine PLO mutant (R219C). This mutant was incubated, with or without added PLO-DS, with sheep red cell membranes to induce oligomerization. The membranes were then solubilized with deoxycholic acid before application to a Sephacryl S-400 column. Oligomers formed from an equimolar mixture of PLO-DS and the active toxin elute between the monomeric toxin and oligomers formed from the active toxin mutant alone (Figure 5). Since the fluorescence signal tracks the labeled active mutant only, the retarded elution indicates that the disulfide mutant indeed causes the active toxin to end up in oligomers of reduced size.

FRET experiments combining N90C-fluorescein and the rhodamine-labeled triple mutant show an efficiency of FRET (Figure 4C) that is intermediate between those of the active (Figure 4A) and inactive (Figure 4B) mutants alone, indicating that the two proteins become incorporated into hybrid oligomers, although the formation of these hybrids appears to be less efficient than the oligomerization of active toxin alone. When wild type PLO or the unlabeled disulfide mutant is added to a mixture of N90C-fluorescein and N90C-rhodamine, they reduce FRET between the two labeled species, indicating the intercalation of unlabeled molecules between the labeled ones in hybrid oligomers (Figure 4D). This effect is greater with wild type toxin than with PLO-DS.

Nevertheless, the result shows that PLO-DS in hybrid oligomers is not restricted to terminal positions, and therefore that its incorparation does not terminate the growth of a hybrid oligomer.

Membrane insertion of active subunits in hybrid oligomers. With the disulfide mutant of PLO, it was shown that the loss of hemolytic activity correlated with the lacking insertion of the two β-hairpins in domain 3 into the membrane (8). From the observation of hybrid oligomers forming between active PLO and PLO-DS, the question arise to what extent the active protein in such hybrids might still undergo membrane insertion. The membrane insertion of the two β-hairpins in domain 3 can be detected by labeling mutant cysteine residues located within them with the environmentally sensitive fluorescent dye nitrobenzoxadiazole (NBD), whose fluorescence emission undergoes a pronounced increase in intensity and excited state lifetime, and a blue shift upon transition from an aqueous to a non-polar environment (7). The insertion of hybrids was studied using the NBD-labeled mutants K231C and A329C, whose cysteine residues are located the first and second hairpin, respectively. When either NBD-labeled mutant was mixed with a twofold excess of the unlabeled PLO-DS, the NBD fluorescence emission was reduced significantly compared to samples that were prepared in the same manner but with unlabeled PLO-WT instead of PLO-DS (Figure 6). However, in both cases, the NBD fluorescence was still well above of that observed with the equivalent amount of toxin not incubated with membranes. The steady-state spectra are in line with time-resolved fluorescence measurements. For mutant K231C, the average excited state lifetime of NBD was was 4.0 ns when mixed with wild type toxin, 3.2 ns when mixed with disulfide mutant, and 1.7 ns in the absence of membranes. For A329C, the lifetimes were 6.2 ns, 2.9 ns, and 2.1 ns, respectively. These findings indicate that PLO-DS inhibits but does not completely abrogate membrane insertion of wild type PLO in hybrid oligomers.

Hemolytic activity of wild type PLO and PLO-DS mixtures. The above observation of partial membrane insertion of oligomers formed from mixtures of active PLO and PLO-DS suggests that such mixtures should retain some hemolytic activity. This is indeed observed. The hemolytic activity of a given amount of wild type PLO is slightly reduced in the presence of an equal amount of PLO-DS, and moderately so with a twofold excess of PLO-DS. In contrast, when PLO-DS is present in fourfold, it very strongly inhibits hemolysis (Figure 7).

Reduction of average pore size by PLO-DS. When PLO-DS is combined with active PLO, it is likely that only a small fraction of all resulting oligomers will not contain any PLO-DS at all. This suggests that the remaining extent of membrane insertion and pore formation observed with such mixtures is at least in part associated with hybrid oligomers. Since these hybrid oligomers are reduced in size, the pores associated with them should be smaller than those formed by full-size, ring-shaped oligomers formed by wild type PLO alone.

Differences in functional pore size can be studied in hemolytic assays using osmotic protection. In this method, the extracellular medium is supplemented with inert macromolecular solutes such as dextran that counteract the osmotic activity of the intracellular hemoglobin. When pore formation occurs, hemolysis will result only if the pores are large enough to permit equilibration of the macromolecular solutes across the membrane, so that they no longer maintain the balance with hemoglobin. On the other hand, if the effective diameter of the protecting solutes exceeds that of the pores, the solutes will remain excluded from the cell and continue to protect it from osmotic lysis. Differential protection by macromolecular solutes varying in size can be used to characterize the pore size.

In the experiment shown in Figure 8A, wild type PLO was incubated with red cells without dextran 6 and dextran 40, respectively. The dextrans cause only a very slight delay in the time course of hemolysis. This is consistent with the fact that the hydrodynamic diameters of dextran 6 (M_r 6000) and dextran 40 (M_r 6000), at approximately 3 and 10 nm, respectively (16), are smaller than the diameter of ring-shaped PLO oligomers (1) and therefore do not afford osmotic protection against the latter.

The picture changes, however, when the wild type PLO is supplemented with one (Figure 8B) or two (Figure 8C) equivalents of disulfide mutant. Here, the time course of hemolysis is markedly slowed by dextran 6, and even more so by the larger dextran 40. This divergence indicates that some of the pores are no longer permeable to the dextran molecules, or else that they are sufficiently reduced in size to significantly slow down the permeation of dextran. On the other hand, with both dextran 6 and dextran 40, hemolysis ultimately occurs, which means that at least some pores are still large enough to allow permeation of dextran. The pores formed by the mixtures of PLO-WT and PLO-DS therefore are heterogeneous in size yet smaller than those

formed by wild type PLO alone. This supports the conclusion that oligomers that contain both wild type PLO and PLO-DS can insert into the membrane and form pores. It confirms the previous contention that incomplete, arc-shaped oligomers can indeed form functional trans-membrane pores (17).

Discussion

The results of this study show a remarkable and surprising difference between the disulfide-tethered PLO mutant and the homologous mutant previously described for perfringolysin O (8). Whereas the latter mutant retains the ability to assemble into complete, ring-shaped pre-pores on membranes, PLO-DS does no longer oligomerize on its own. This discrepancy may be related to a subtle yet long-ranging conformational change that is triggered by membrane binding and whose interception by mutagenesis interferes with proper oligomerization (18; 19). It seems possible that the presence of the disulfide bond may interfere with this conformational shift to different extents in PLO and perfringolysin, preventing oligomerization in one case but not the other.

The notion that the difference in the functional defect between the two disulfide mutants is quantitative rather than qualitative is supported by the finding that PLO-DS retains the ability to form hybrid oligomers with wild type PLO. A possible explanation of this observation would be a 'hemiplegic' inactivation of the mutant, such that it can attach to a growing oligomer of wild type molecules using its remaining active oligomerization surface, which would then leave the inactive one exposed and so terminate the further growth of the oligomer. In this case, however, PLO-DS should be confined to one end of a hybrid oligomer and be able to intercalate between active subunits. This is not in line with the observation that unlabeled PLO-DS can significantly reduce FRET between labeled, hemolytically active mutants within hybrid oligomers.

Another possible explanation for the incorporation of PLO-DS into hybrid but not homogeneous oligomers may be related to the existence of different kinetic stages of oligomerization (20). In the rate-limiting initiation reaction, two or more monomers react with one another, and the kinetic handicaps of multiple mutant molecules would likely act additively at this stage. In contrast, in the subsequent extension stage, growing oligomers reacts with further monomers one at a time. In this reaction, kinetic obstruction would only apply to one of the partners and therefore more readily overcome. Nevertheless, even in this situation, oligomerization of PLO-DS is inhibited, resulting in the formation of incomplete, arc-shaped oligomers. Thus, wild type toxin promotes the oligomerization of the disulfide mutant, yet the latter inhibits oligomerization of the former; neither is entirely dominant.

Another interesting finding of this study is the pattern of hemolytic activity and of membrane insertion observed with hybrid oligomers. Mixing wild type PLO and PLO-DS likely produces a distribution of oligomers that differ not only in size but also in composition, with some oligomers containing a higher proportion of the disulfide mutant than others. Some oligomers containing no PLO-DS at all should also form; however, at a twofold excess of PLO-DS over wild type PLO, their number should be small. At this same ratio, approximately 50% of both membrane insertion and hemolytic activity is still preserved. Some of this remaining activity must therefore be associated with hybrid oligomers. This conclusion is supported by the fact that pores formed under these conditions are smaller on average than those formed by wild type toxin only. In contrast, at fourfold or greater excess of PLO-DS, electron microscopy still shows appreciable formation of arc-shaped oligomers, but hemolysis is sharply reduced; most oligomers therefore seem to be arrested at the pre-pore stage.

These results signify that, with respect to membrane insertion as with oligomerization, neither the wild type toxin nor PLO-DS is clearly dominant over the other. Insertion of hybrids formed at moderate proportions of PLO-DS indicates that not all subunits of an oligomer need to participate in its membrane insertion. On the other hand, its suppression by PLO-DS in greater proportion indicates that membrane insertion requires a certain critical proportion of active subunits. Overall, these findings suggest that membrane insertion requires the cooperation of a number of adjacent subunits within the oligomer.

In conclusion, our study provides additional insights into the mechanism of oligomerization and pore formation by CDCs. The initial conformational change that is associated with membrane binding and which sets the stage for oligomerization (ref) involves conformational flexibility between domains 2 and 3. The complementation of PLO-DS oligomerization by wild type PLO supports a two-step model of oligomerization that so far had been based on kinetic modeling only (20). The fact that membrane insertion and pore formation can occur in oligomers that contain some insertion-deficient subunits indicates that the process of insertion is only partially cooperative.

References

1 Bhakdi, S., Tranum-Jensen, J. & Sziegoleit, A. (1985). *Infect Immun* **47**, 52-60.

2 Tilley, S.J., Orlova, E.V., Gilbert, R.J.C., Andrew, P.W. & Saibil, H.R. (2005). *Cell* **121**, 247-256.

3 Rossjohn, J., Feil, S., McKinstry, W., Tweten, R. & Parker, M. (1997). *Cell* **89**, 685-692.

4 Polekhina, G., Giddings, K.S., Tweten, R.K. & Parker, M.W. (2005). *Proc Natl Acad Sci U S A* **102**, 600-605.

5 Shepard, L., Shatursky, O., Johnson, A. & Tweten, R. (2000). *Biochemistry* **39**, 10284-10293.

6 Palmer, M., Saweljew, P., Vulicevic, I., Valeva, A., Kehoe, M. & Bhakdi, S. (1996). *J Biol Chem* **271**, 26664-26667.

7 Shatursky, O., Heuck, A., Shepard, L., Rossjohn, J., Parker, M., Johnson, A. & Tweten, R. (1999). *Cell* **99**, 293-299.

8 Hotze, E., Wilson-Kubalek, E., Rossjohn, J., Parker, M., Johnson, A. & Tweten, R. (2001). *Journal of Biological Chemistry* **276**, 8261-8268.

9 Billington, S.J., Jost, B.H., Cuevas, W.A., Bright, K.R. & Songer, J.G. (1997). *J Bacteriol* **179**, 6100-6106.

10 Howorka, S. & Bayley, H. (1998). *Biotechniques* **25**, 764-6, 768, 770 passim.

11 Harris, J., Adrian, M., Bhakdi, S. & Palmer, M. (1998). *J Struct Biol* **121**, 343-355.

12 Harris, J. (1997). **35**, .

13 Duncan, J.L. & Schlegel, R. (1975). *J Cell Biol* **67**, 160-174.

14 Wu, P. & Brand, L. (1994). *Anal Biochem* **218**, 1-13.

15 Harris, R.W., Sims, P.J. & Tweten, R.K. (1991). *J Biol Chem* **266**, 6936-6941.

16 Scherrer, R. & Gerhardt, P. (1971). *J Bacteriol* **107**, 718-735.

17 Palmer, M., Harris, R., Freytag, C., Kehoe, M., Tranum-Jensen, J. & Bhakdi, S. (1998). *EMBO J* **17**, 1598-1605.

18 Abdel Ghani, E.M., Weis, S., Walev, I., Kehoe, M., Bhakdi, S. & Palmer, M. (1999). *Biochemistry* **38**, 15204-15211.

19 Ramachandran, R., Tweten, R. & Johnson, A. (2004). *Nature Structural and Molecular Biology* **11**, 697-705.

20 Palmer, M., Valeva, A., Kehoe, M. & Bhakdi, S. (1995). *Eur J Biochem* **231**, 388-395.

Figure Legends

Figure 1: Structure of PLO (homology model, based on the crystal structure of perfringolysin O (3)). The positions of the engineered disulfide bridge between residues 85 in domain 2 and 219 in domain 3, as well as those of the additional cysteine mutations employed in this study are indicated.

Figure 2: Hemolytic activity of reduced and unreduced PLO-DS and of wild type PLO. Sheep RBC (0.5% in PBS) were incubated with the indicated amounts of PLO-WT or PLO-DS and incubated at 37 ºC for 30 minutes. The OD_{650} reflects the fraction of cells that remain intact after the incubation; hemolysis is apparent as a drop in the OD_{650}.

Figure 3: Electron microscopy of wild type PLO and of PLO-DS, alone and in mixtures, on cholesterol crystals (negative staining with 2% uranyl acetate). The protein (0.125 mg/ml) and cholesterol crystals (0.5 mg/ml) were incubated for 30 minutes at room temperature. A: Wild type PLO, B: PLO-DS, C: Wild type PLO and PLO-DS 1:1, D: Wild type PLO and PLO-DS 1:10.

Figure 4: FRET experiments on the oligomerization of PLO-DS. The active single cysteine mutant N90C and the triple mutant PLO-DS-K328C were labeled with fluorescein (F) or rhodamine (R), respectively. The labeled proteins were incubated with membranes, and the fluorescence emission was recorded with excitation at 465 nm. Solid lines represent spectra of equimolar mixtures of fluorescein- and rhodamine-labeled proteins; dashed lines represent spectra of the fluorescein-labeled proteins only. A: Oligomerization of the active mutant N90C is evident by the suppression of fluorescein emission due to FRET to rhodamine. B: The triple mutant does not show significant FRET, indicating lack of oligomerization. C: FRET between N90C-F and rhodamine-labeled triple mutant indicates formation of hybrid oligomers. D: FRET between N90C-F and N90C-R in the presence of unlabeled PLO-DS or wild type PLO. The amount of unlabeled protein equaled the total of the labeled species.

Figure 5: Reduced size of hybrid oligomers, detected by gel filtration. The active mutant R219C was labeled with fluorescein. To induce oligomerization, the mutant was incubated with membranes alone (hollow squares) or as a mixture with an equal amount of unlabeled PLO-DS.

The membranes were solubilized with deoxycholate, and the oligomers were applied to a Sephacryl S400 column. The fluorescence of the eluate fractions was measured to detect the labeled protein. For comparison, a sample of labeled R219C not incubated with membranes is shown (hollow circles).

Figure 6: Membrane insertion of domain 3 in hybrid oligomers. Mutants K213C and A329C were labeled with NBD, and the fluorescence emission was measured in the absence of membranes, and after incubation with membranes either alone or after addition of unlabeled PLO-DS in twofold molar excess. The fluorescence increase after incubation with membranes reflects the extent of membrane insertion of the labeled, active mutants.

Figure 7: Hemolytic activity of mixtures of wild type PLO in mixtures with PLO-DS. For each combination, the amounts of wild type and of PLO-DS are stated as multiples of the equivalents indicated on the x axis. The experimental procedure was as in Figure 2; drop of OD_{650} indicates hemolysis.

Figure 8: Osmotic protection of red cells against mixtures of wild type PLO and PLO-DS by dextran 6 and dextran 40. Wild type PLO (2.5 μg/ml) alone (A) or with the same amount (B) or twice the amount (C) of PLO-DS was incubated in buffer, with or without dextran 6 or dextran 40. The OD_{650} was followed over time; a drop in the OD_{650} indicates hemolysis.

Figure 1

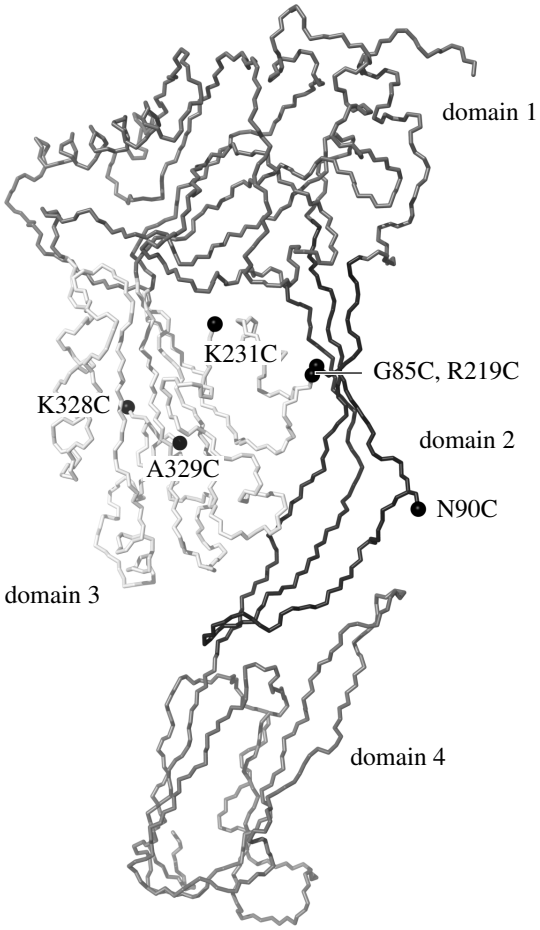
domain 1
K231C
G85C, R219C
K328C
domain 2
A329C
N90C
domain 3
domain 4

Figure 2

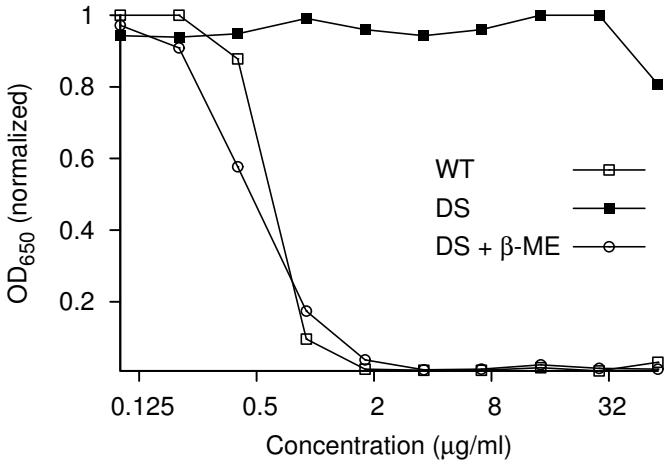
1
0.8
0.6
0.4
0.2
OD650 (normalized)
WT
DS
DS + β-ME
0.125
0.5
2
8
32
Concentration (μg/ml)

Figure 3

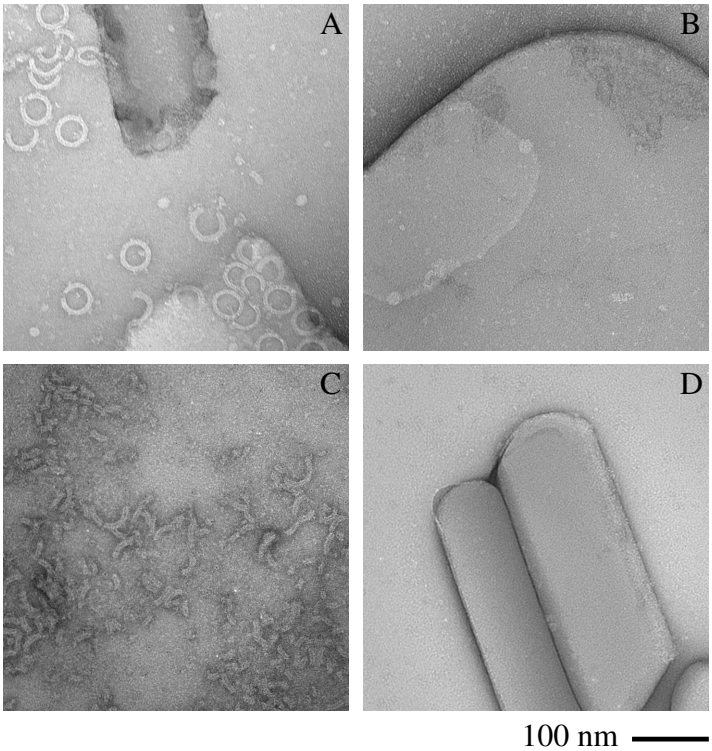

Figure 4

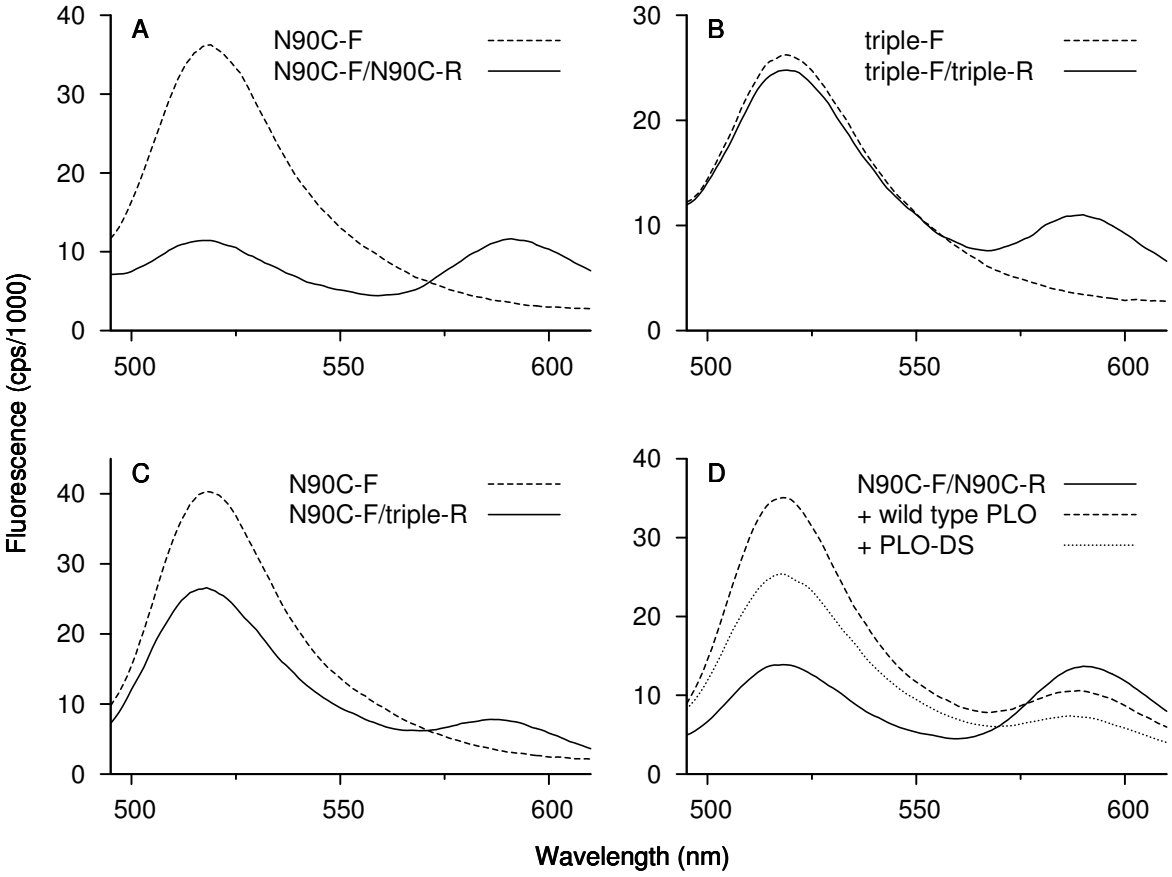
A
N90C-F
N90C-F/N90C-R
B
triple-F
triple-F/triple-R
C
N90C-F
N90C-F/triple-R
D
N90C-F/N90C-R
+ wild type PLO
+ PLO-DS
Fluorescence (cps/1000)
Wavelength (nm)
0
10
20
30
40
500
550
600

Figure 5

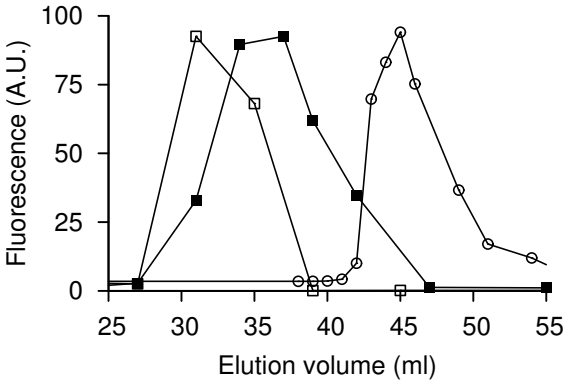
100
75
50
25
0
Fluorescence (A.U.)
25
30
35
40
45
50
55
Elution volume (ml)

Figure 6

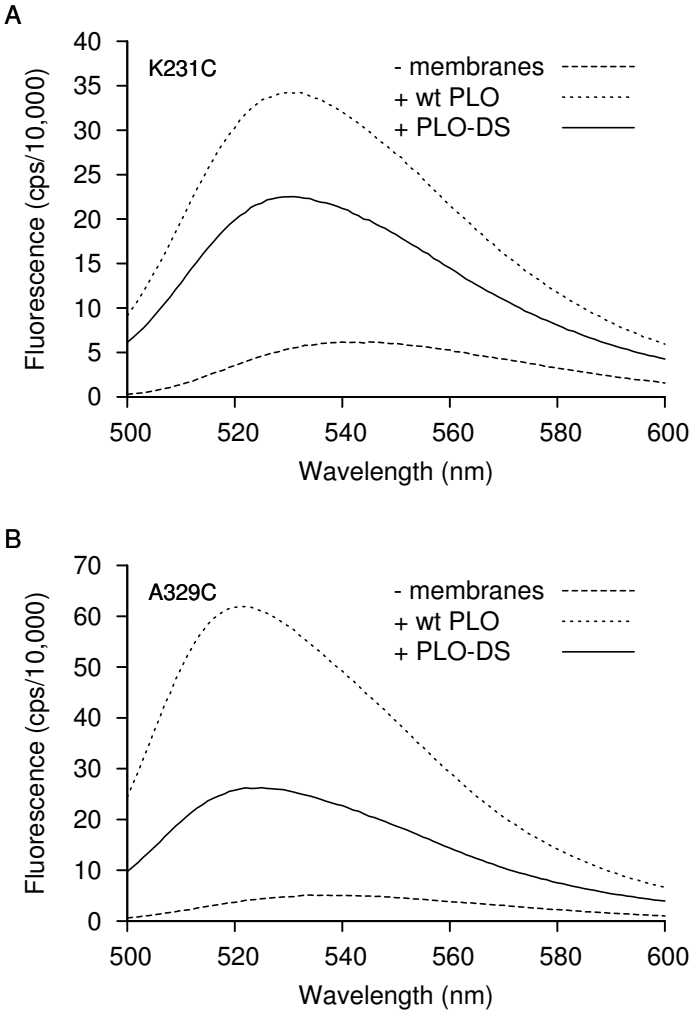
A
K231C
- membranes
+ wt PLO
+ PLO-DS
Fluorescence (cps/10,000)
0
5
10
15
20
25
30
35
40
500
520
540
560
580
600
Wavelength (nm)
B
A329C
- membranes
+ wt PLO
+ PLO-DS
Fluorescence (cps/10,000)
0
10
20
30
40
50
60
70
500
520
540
560
580
600
Wavelength (nm)

Figure 7

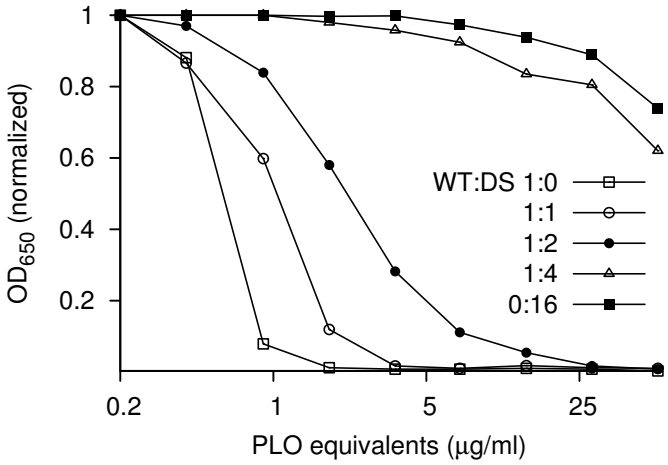
1
0.8
0.6
0.4
0.2
OD650 (normalized)
WT:DS 1:0
1:1
1:2
1:4
0:16
0.2
1
5
25
PLO equivalents (µg/ml)

Figure 8

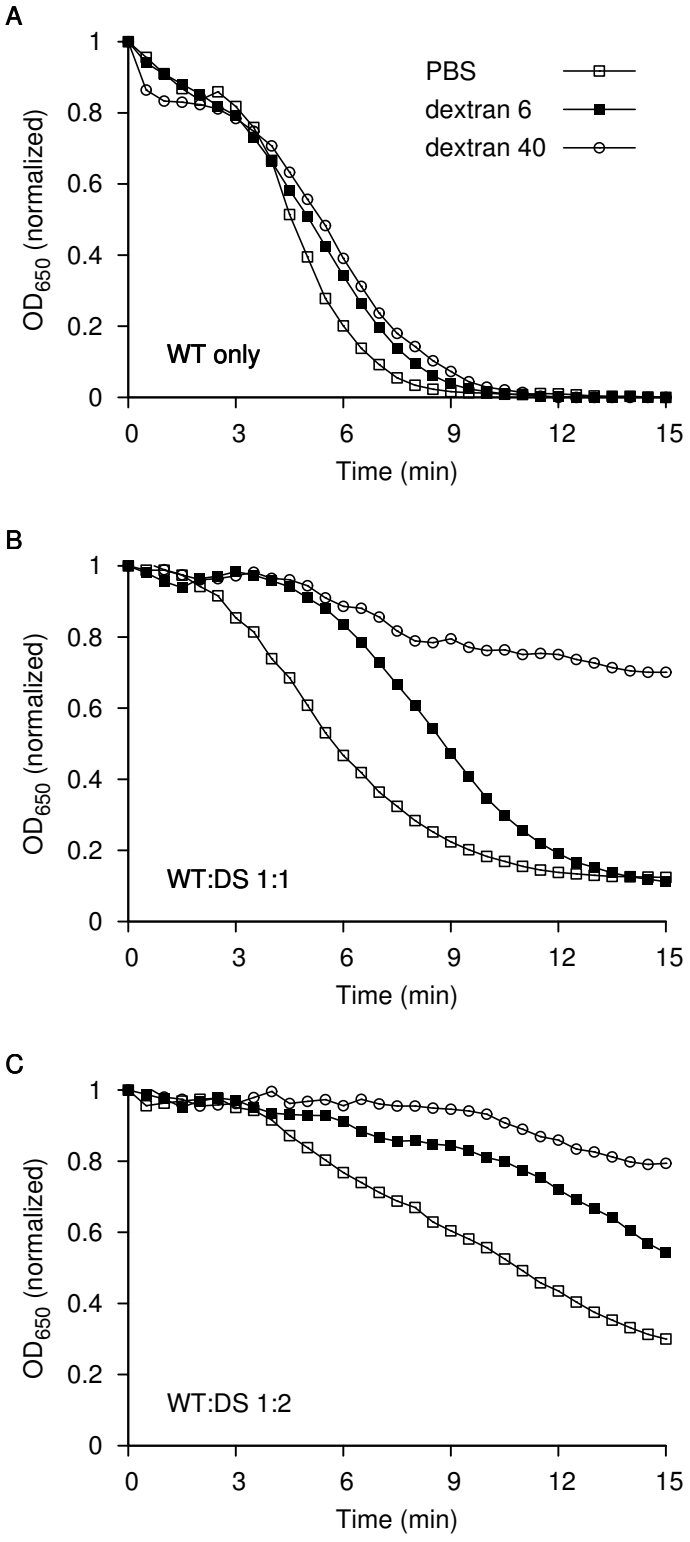
A
PBS
dextran 6
dextran 40
WT only
OD650 (normalized)
Time (min)
B
WT:DS 1:1
OD650 (normalized)
Time (min)
C
WT:DS 1:2
OD650 (normalized)
Time (min)